

# 15. HIGH-RESOLUTION, WHOLE-CORE MAGNETIC SUSCEPTIBILITY LOGS FROM LEG 108<sup>1</sup>

J. Bloemendal,<sup>2</sup> L. Tauxe,<sup>3</sup> J.-P. Valet,<sup>4</sup>  
and  
Shipboard Scientific Party<sup>5</sup>

## ABSTRACT

We present high-resolution (3- to 20-cm interval) whole-core magnetic susceptibility logs for Sites 657 through 661 and Sites 665 through 668 cored during Leg 108. These logs provide the potential for detailed within-site correlation of offset holes, and by reflecting variations in the concentration of terrigenous material also may be significant for environmental studies.

## INTRODUCTION

During Leg 108 we tried routinely to obtain high-resolution (3- to 20-cm intervals) magnetic-susceptibility logs from whole cores of the recovered sediment. Our main objective was to use these data for obtaining detailed within-site correlations between holes. This would enable us to generate a stratigraphically "complete" composite section from two or more offset holes at a site by bypassing core breaks, other disturbed intervals, and intervals with no recovery. The value of whole-core susceptibility logging for rapid correlation of lake-sediment sections has been demonstrated (e.g., Thompson et al., 1975; Bloemendal et al., 1979), but so far this technique has not been used much for correlating marine sediments. Because susceptibility records from deep-sea sediments frequently reflect variations in the concen-

tration of terrigenous material, they also may be useful for paleoenvironmental studies (e.g., Kent, 1982; Robinson, 1986). Between-hole correlations for Leg 108 sites are given in individual site chapters (this volume). This chapter provides the down-hole plots of all whole-core susceptibility logs obtained during Leg 108 and enables us to assess the character and quality of the records. This chapter complements contributions from P. Schultheiss, J. Mienert, and Shipboard Scientific Party members (this volume), which provide downhole plots of both whole-core, P-wave velocity and GRAPE density logs.

## INSTRUMENTATION AND METHODS

Measurements were performed using the shipboard Bartington Instruments MS1 susceptibility meter, interfaced with a DEC PRO 350 microcomputer, together with an 8-cm inside diameter Bartington Instruments MS1CX whole-core scanning sensor that generated a 0.34-mT alternating field with a frequency of 147 Hz. The sensitivity of the instrument is about  $10 \times 10^{-6}$  SI units. Figure 1 shows the response of this sensor to the horizontal displacement of a thin, discoidal stratum 6.8 cm in diameter. We used a point of 66% signal attenuation to estimate the effective volume of sediment contributing to the susceptibility signal (about 80 cm<sup>3</sup>). The results obtained using this assumption were comparable to the results obtained from subsequent volume susceptibility measurements of discrete samples.

During laboratory operation, unsplit cores were pushed manually through the sensor, and measurements performed at intervals of from 3 to 20 cm, depending upon time available and the observed frequency of susceptibility variations. We could measure one 9.5-m-long core in 3-cm intervals in about 1 hr. Data for each core section were stored on floppy diskettes, transferred to the shipboard VAX 11/750 computer, and plotted on a Hewlett-Packard 7475A graph plotter. This procedure could be improved significantly by automating the passage of the cores through the susceptibility sensor and by providing a dedicated graph plotter so that results for each core could be displayed immediately after measuring. Depths below the seafloor (mbsf) were estimated by assuming that the top of each hole was 0 mbsf. Subsequent depths were calculated from the core and section length, and data were filed routinely on the VAX 11/750 computer.

## RESULTS

Figures 2 through 16 show the whole-core susceptibility logs. The log for each hole is divided into 30-m intervals; voids of 1 m long or greater are denoted by a vertical line terminated by horizontal bars.

<sup>1</sup> Ruddiman, W., Sarnthein, M., Baldauf, J., et al., 1988. *Proc., Init. Repts. (Pt. A), ODP*, 108.

<sup>2</sup> Graduate School of Oceanography, University of Rhode Island, Narragansett, RI 02882.

<sup>3</sup> Scripps Institution of Oceanography, La Jolla, CA 92093.

<sup>4</sup> Centre des Faibles Radioactivités, CNRS, Avenue de la Terrasse, 91190 Gif-sur-Yvette, France.

<sup>5</sup> William Ruddiman (Co-Chief Scientist), Lamont-Doherty Geological Observatory, Palisades, NY 10964; Michael Sarnthein (Co-Chief Scientist), Geologisch-Paläontologisches Institut, Universität Kiel, Olshausenstrasse 40, D-2300 Kiel, Federal Republic of Germany; Jack Baldauf, ODP Staff Scientist, Ocean Drilling Program, Texas A&M University, College Station, TX 77843; Jan Backman, Department of Geology, University of Stockholm, S-106 91 Stockholm, Sweden; Jan Bloemendal, Graduate School of Oceanography, University of Rhode Island, Narragansett, RI 02882-1197; William Curry, Woods Hole Oceanographic Institution, Woods Hole, MA 02543; Paul Farrimond, School of Chemistry, University of Bristol, Cantocks Close, Bristol BS8 1TS, United Kingdom; Jean Claude Faugeres, Laboratoire de Géologie-Océanographie, Université de Bordeaux I, Avenue des Facultés, Talence 33405, France; Thomas Janacek, Lamont-Doherty Geological Observatory, Palisades, NY 10964; Yuzo Katsura, Institute of Geosciences, University of Tsukuba, Ibaraki 305, Japan; Hélène Manivit, Laboratoire de Stratigraphie des Continents et Océans, (UA 319) Université Paris VI, 4 Place Jussieu, 75230 Paris Cedex, France; James Mazzullo, Department of Geology, Texas A&M University, College Station, TX 77843; Jürgen Mienert, Geologisch-Paläontologisches Institut, Universität Kiel, Olshausenstrasse 40, D-2300 Kiel, Federal Republic of Germany, and Woods Hole Oceanographic Institution, Woods Hole, MA 02543; Edward Pokras, Lamont-Doherty Geological Observatory, Palisades, NY 10964; Maureen Raymo, Lamont-Doherty Geological Observatory, Palisades, NY 10964; Peter Schultheiss, Institute of Oceanographic Sciences, Brook Road, Wormley, Godalming, Surrey GU8 5UG, United Kingdom; Rüdiger Stein, Geologisch-Paläontologisches Institut, Universität Giessen, Senckenbergstrasse 3, 6300 Giessen, Federal Republic of Germany; Lisa Tauxe, Scripps Institution of Oceanography, La Jolla, CA 92093; Jean-Pierre Valet, Centre des Faibles Radioactivités, CNRS, Avenue de la Terrasse, 91190 Gif-sur-Yvette, France; Philip Weaver, Institute of Oceanographic Sciences, Brook Road, Wormley, Godalming, Surrey GU8 5UG, United Kingdom; Hisato Yasuda, Department of Geology, Kochi University, Kochi 780, Japan.

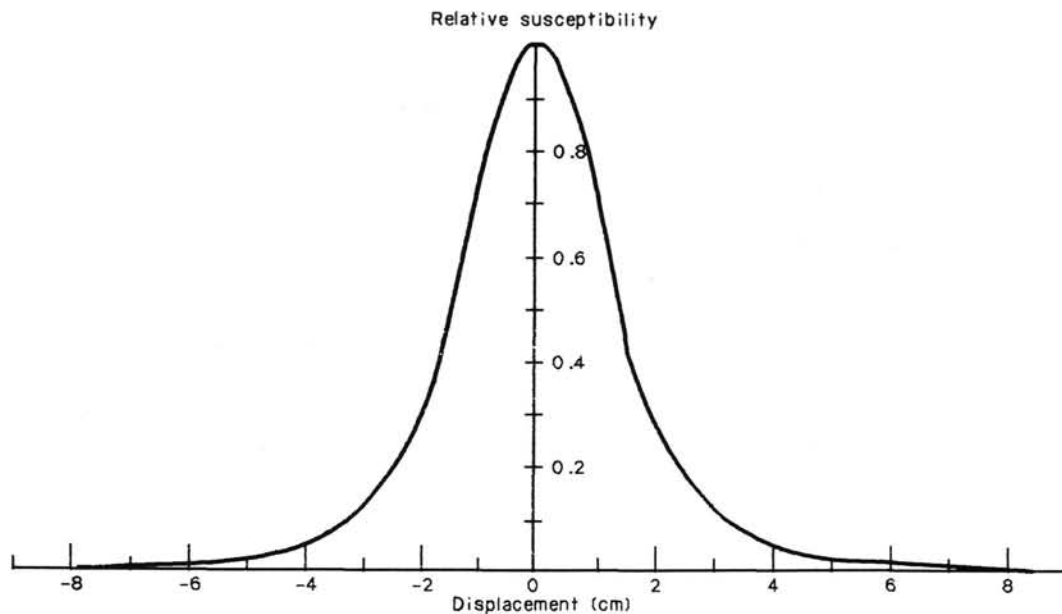


Figure 1. Response of the Bartington Instruments MS1CX susceptibility sensor to the horizontal displacement of a thin, discoidal stratum 6.8 cm in diameter.

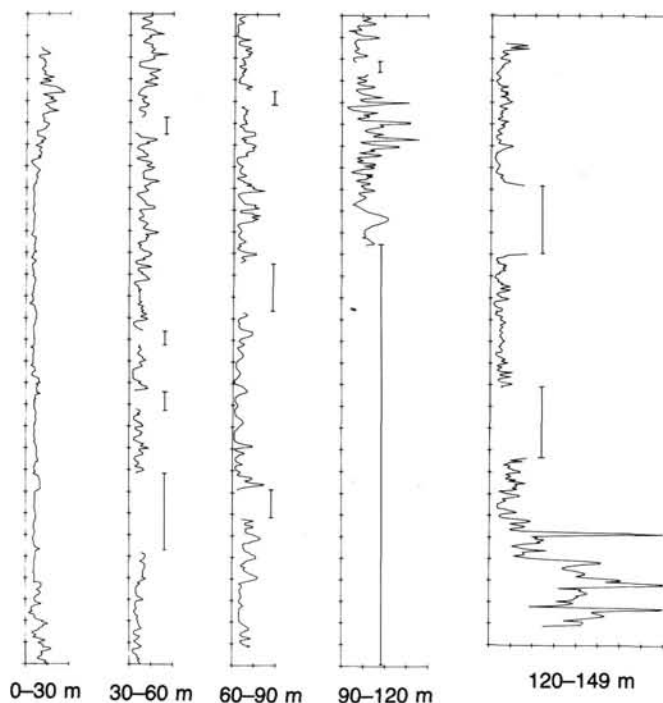


Figure 2. Whole-core magnetic susceptibility log for Hole 657A. In this, and in all subsequent logs, the increment for the depth axis is 1 m and that for the susceptibility axis is  $100 \times 10^{-6}$  SI units of volume susceptibility.

Measurements generally were confined to advanced piston corer (APC) cores. Extended-core barrel (XBC) cores were highly disturbed, and significant variations in the diameter of the sediment column occurred within the core liner and, hence, in the

volume of material contributing to the susceptibility signal. At Site 658, we could obtain reliable measurements only from about the upper 10 cores because of the numerous voids in subsequent cores generated by the presence of significant volumes of free gas. At Sites 662 through 664, susceptibilities generally were low (less than about  $50 \times 10^{-6}$  SI units), and patterns of variation could not be repeated between cores covering the same below seafloor depth intervals. We concluded that the obtained results reflected a combination of the intrinsic magnetic properties of the core liners and any contaminants introduced during coring. In Hole 666A, the 150-m sequence that was cored contained numerous turbidite sands, and the second, offset, hole was cancelled. Consequently, susceptibility measurements were terminated before reaching the base of the hole.

#### ACKNOWLEDGMENTS

We thank the following members of the Shipboard Scientific and Technical Party: John Tauxe, who helped set up the whole-core susceptibility logging system and who provided interest and enthusiasm throughout; Dan Bontempo, who provided invaluable computing assistance; and Bill Curry, Tom Janacek, Yuso Katsura, Ed Pokras, Maureen Raymo, Kevin Rodgers, and Bill Ruddiman, who helped with the exceptionally tedious job of performing the measurements.

#### REFERENCES

Bloemendal, J., Oldfield, F., and Thompson, R., 1979. Magnetic measurements used to assess sediment influx in Llyn Goddionduon. *Nature*, 280:50-51.  
 Kent, D. V., 1982. Apparent correlations of palaeomagnetic intensity and climatic records in deep-sea sediments. *Nature*, 299:538-539.  
 Robinson, S. G., 1986. The late Pleistocene palaeoclimatic record of North Atlantic deep-sea sediments revealed by mineral-magnetic measurements. *Phys. Earth Planet. Inter.*, 42:22-47.  
 Thompson, R., Battarbee, R. W., O'Sullivan, P. E., and Oldfield, F., 1975. Magnetic susceptibility of lake sediments. *Limnol. Oceanogr.*, 20:687-698.

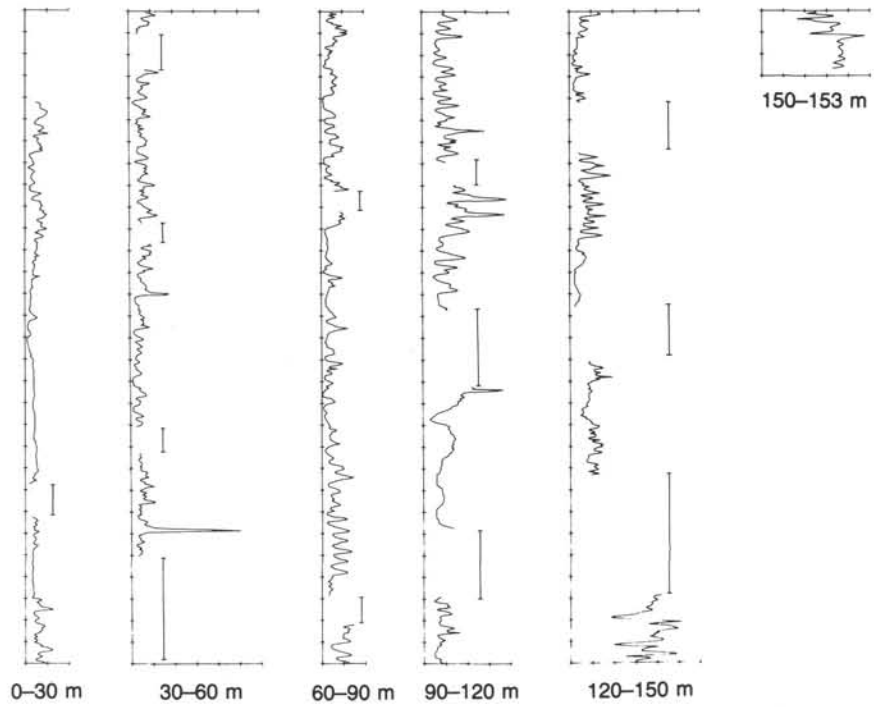


Figure 3. Whole-core magnetic susceptibility log for Hole 657B.

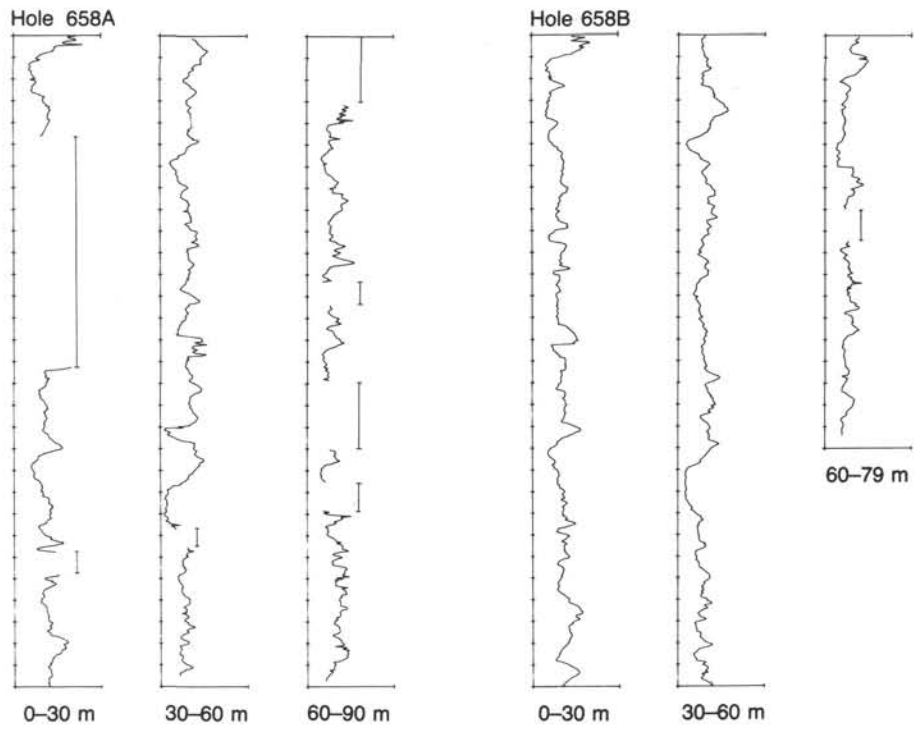


Figure 4. Whole-core magnetic susceptibility logs for Holes 658A and 658B.

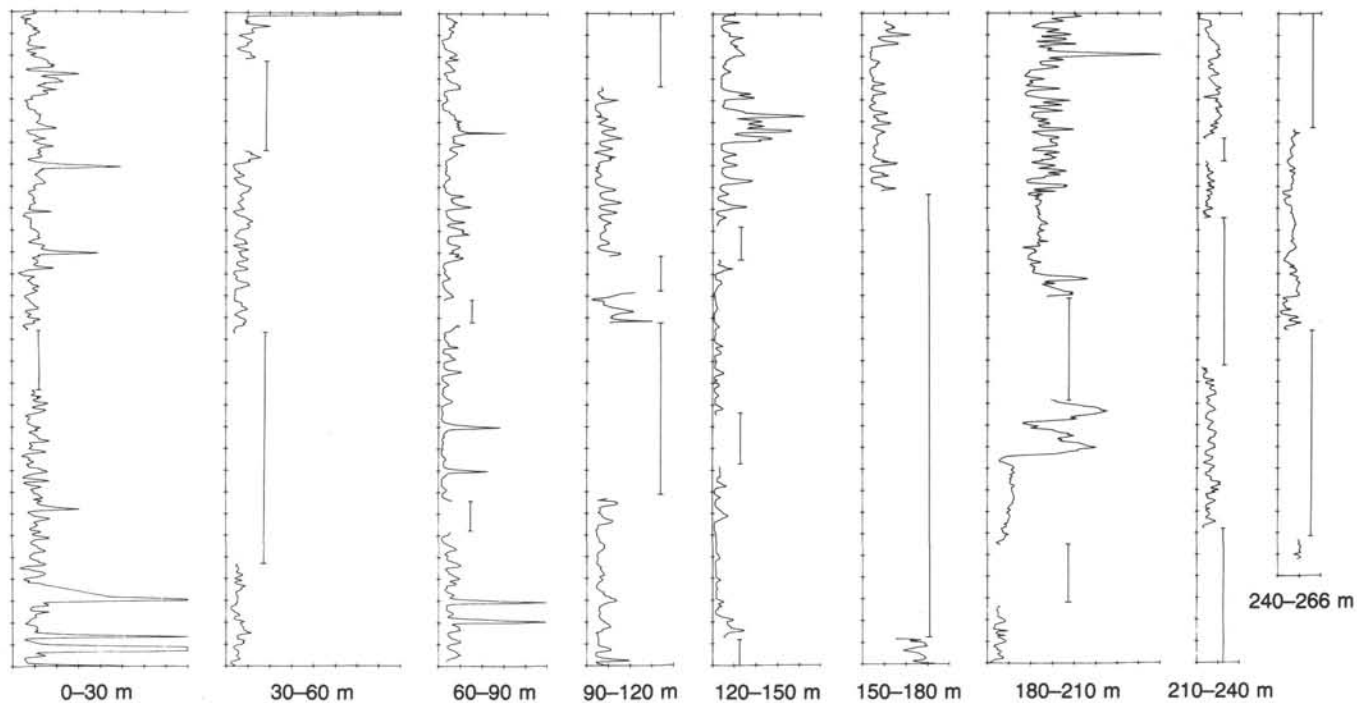


Figure 5. Whole-core magnetic susceptibility log for Hole 659A.

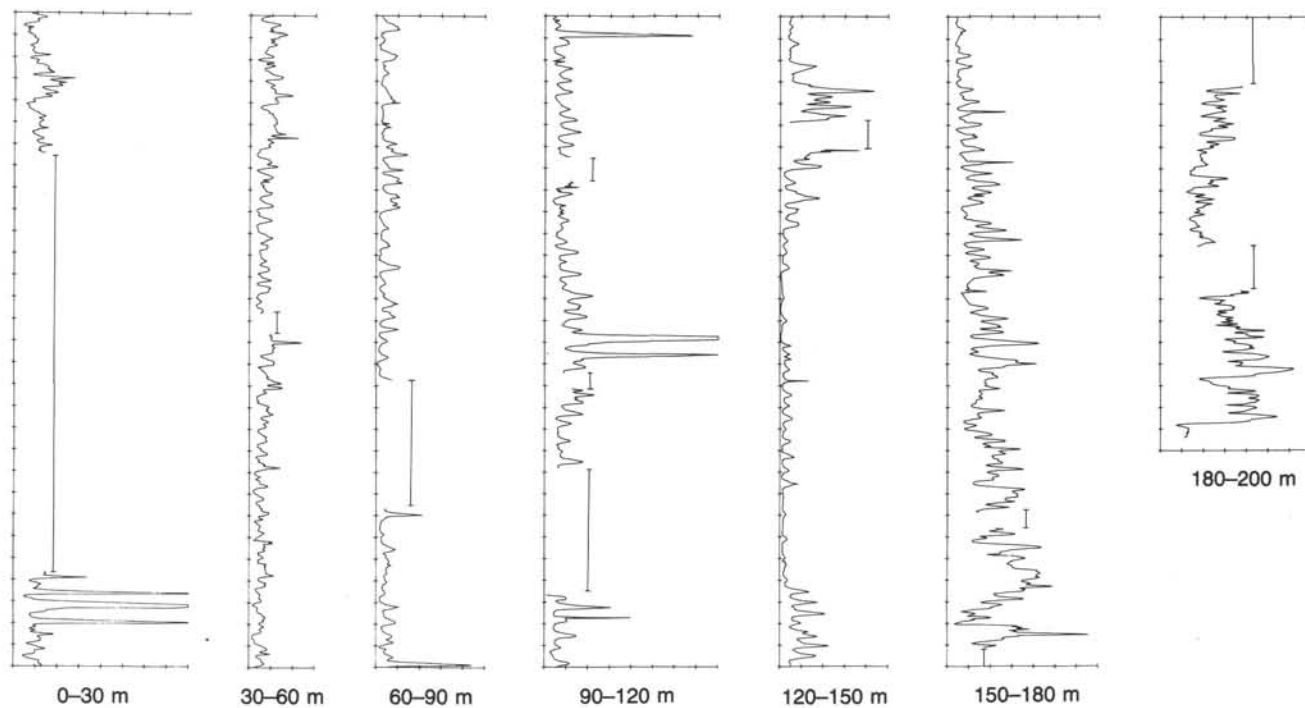


Figure 6. Whole-core magnetic susceptibility log for Hole 659B.

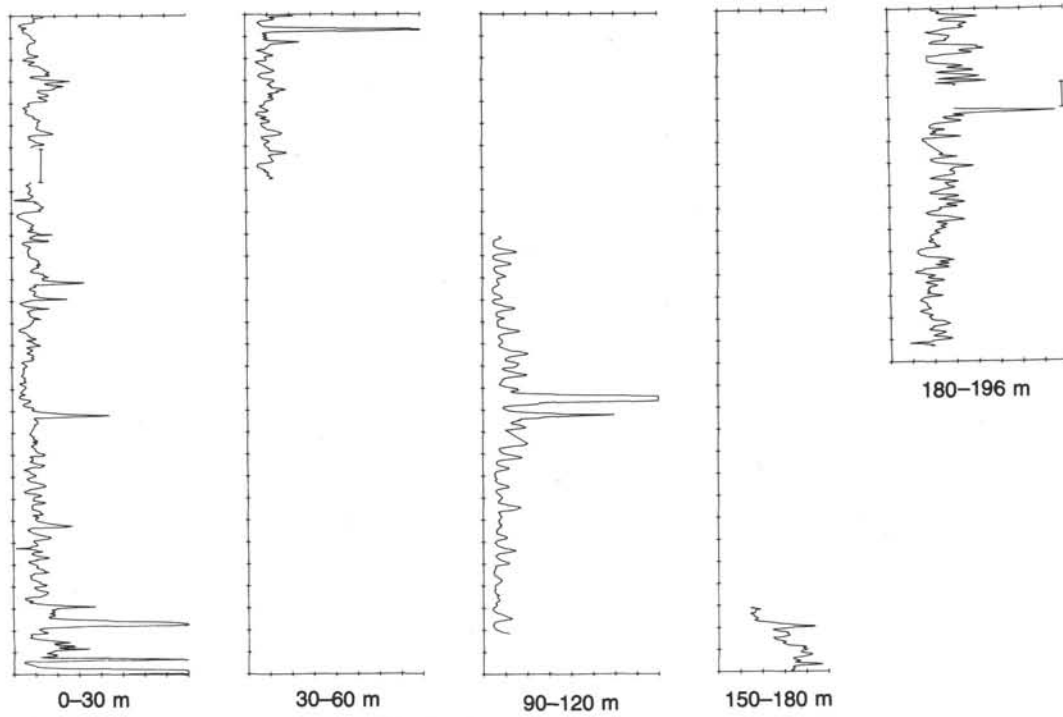


Figure 7. Whole-core magnetic susceptibility log for Hole 659C.

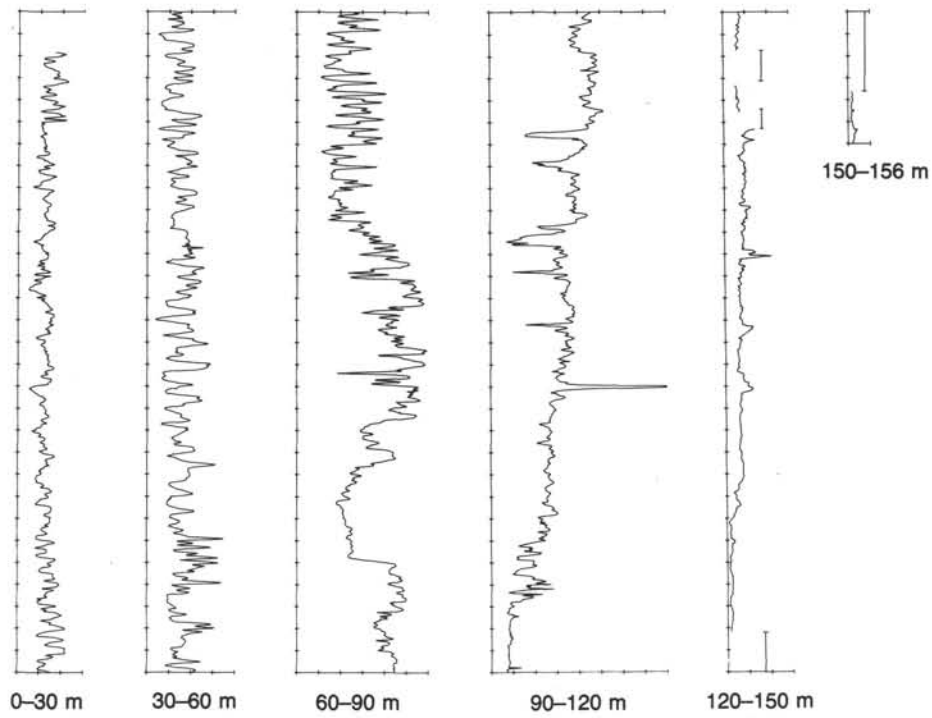


Figure 8. Whole-core magnetic susceptibility log for Hole 660A.

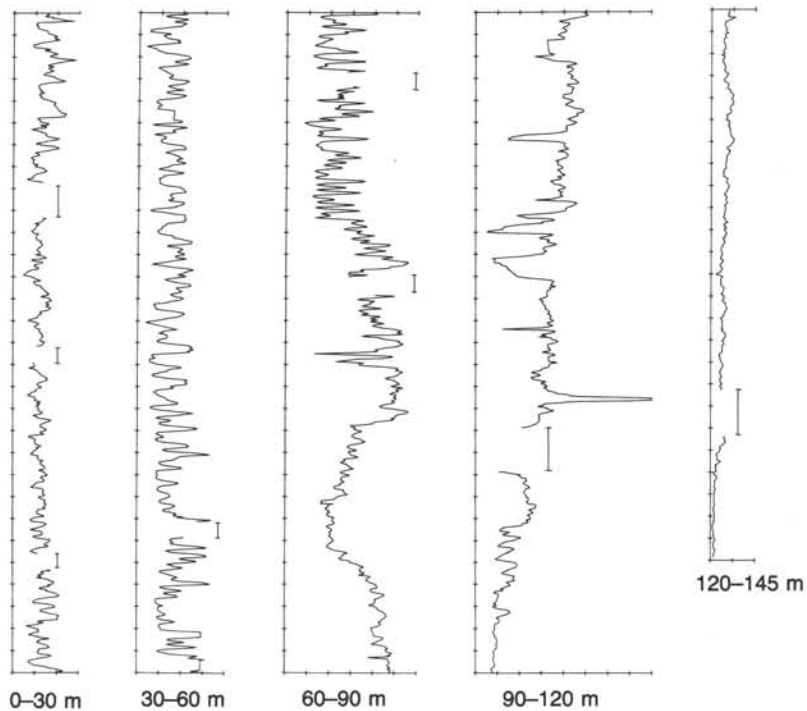


Figure 9. Whole-core magnetic susceptibility log for Hole 660B.

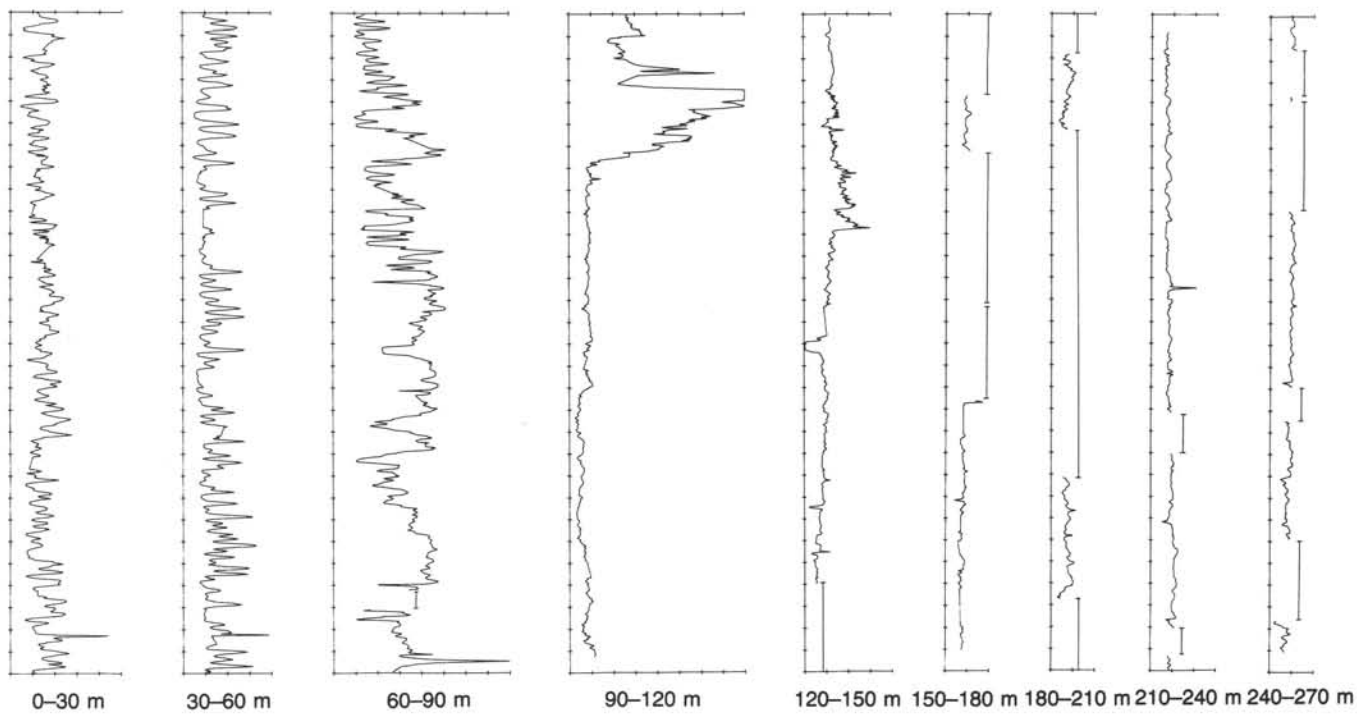


Figure 10. Whole-core magnetic susceptibility log for Hole 661A.

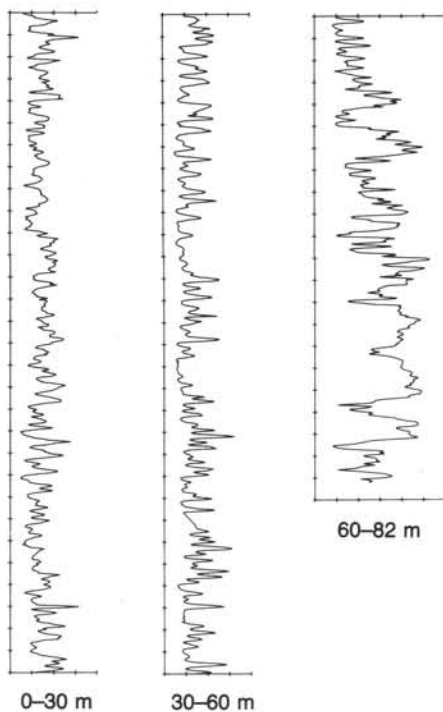


Figure 11. Whole-core magnetic susceptibility log for Hole 661B.

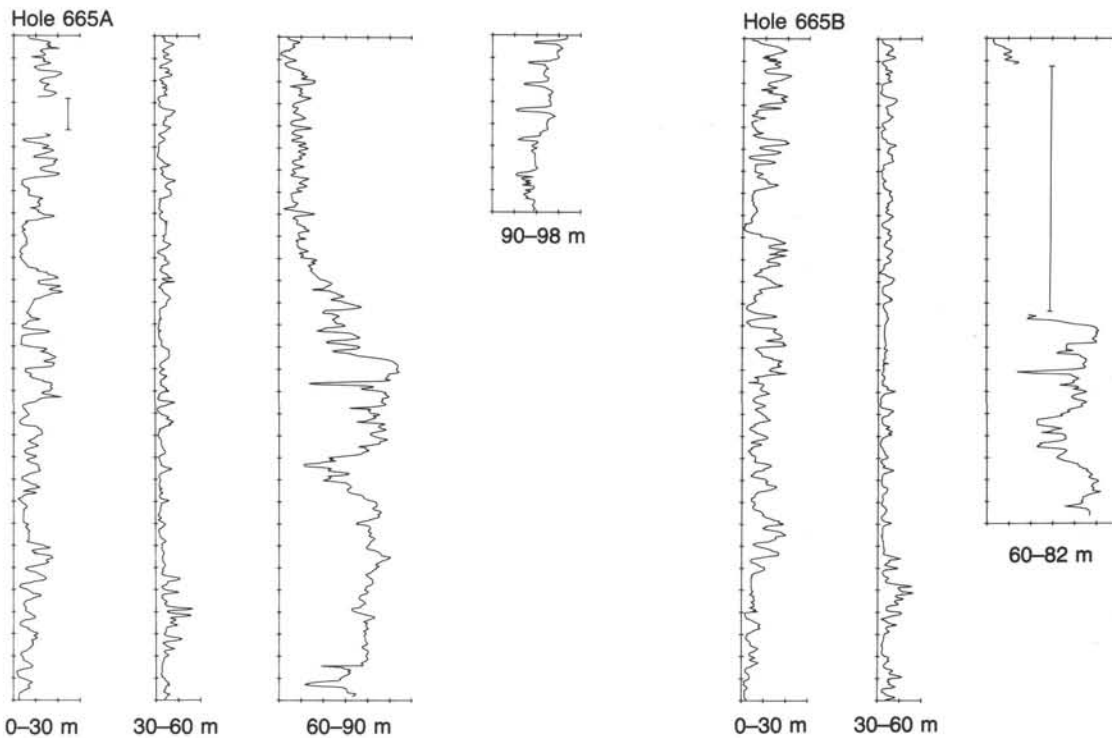


Figure 12. Whole-core magnetic susceptibility logs for Holes 665A and 665B.



Figure 13. Whole-core magnetic susceptibility log for Hole 666A.

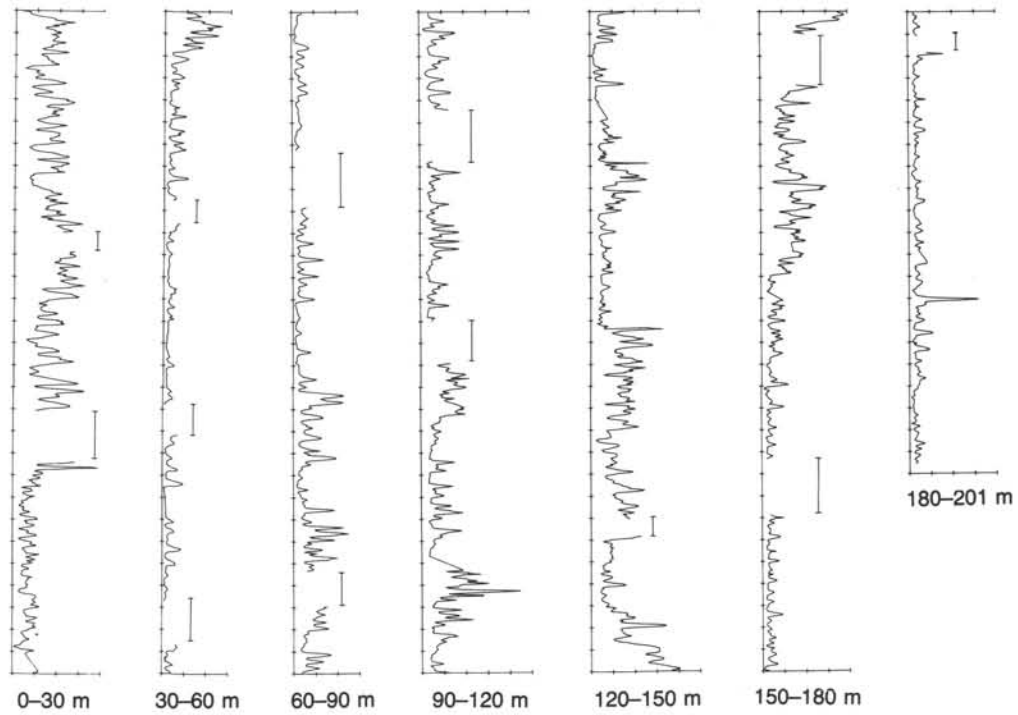


Figure 14. Whole-core magnetic susceptibility log for Hole 667A.



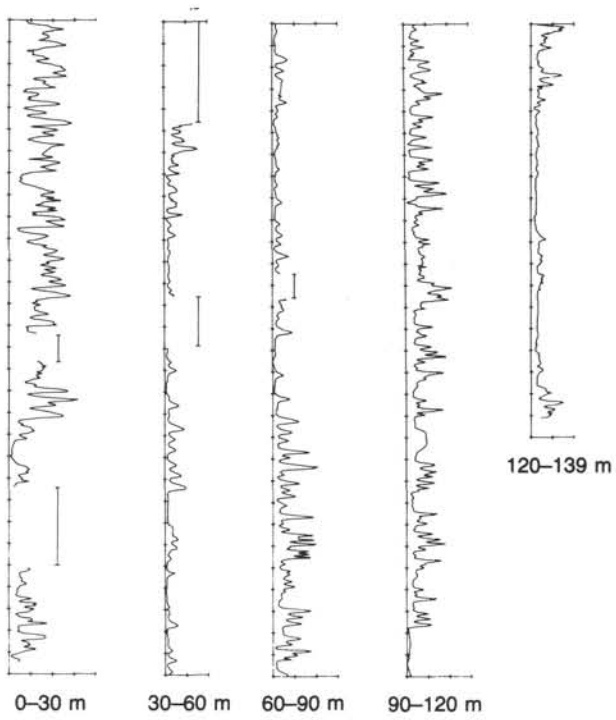


Figure 15. Whole-core magnetic susceptibility log for Hole 667B.

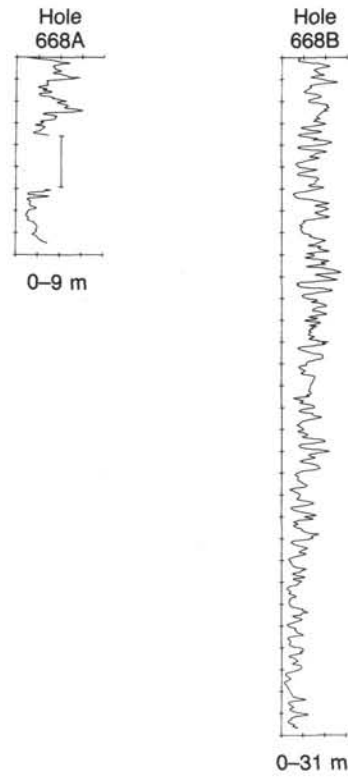


Figure 16. Whole-core magnetic susceptibility logs for Holes 668A and 668B.